# SUPERCRITICAL INJECTION OF CRYOGENIC NITROGEN JET

**N. M. Kuznetsov**[1], **S. N. Medvedev**[1], **S. M. Frolov**[1,2,3], **F. S. Frolov**[1,3], **B. Basara**[4], **and K. Pachler**[4]

[1]N. N. Semenov Federal Research Center for Chemical Physics of the Russian Academy of Sciences
4 Kosigin Str., Moscow 119991, Russian Federation
e-mail: smfrol@chph.ras.ru
[2]National Research Nuclear University MEPhI
31 Kashirskoe Sh., Moscow 115409, Russian Federation
[3]Federal State Institution "Scientific Research Institute for System Analysis of the Russian Academy of Sciences"
36-1 Nakhimovskii Prosp., Moscow 117218, Russian Federation
[4]AVL LIST GmbH, Graz, Austria

Using the wide-range real-gas equation of state (EOS) of nitrogen, the gasdynamic calculations of the supercritical injection of a submerged turbulent jet of cryogenic nitrogen into a chamber filled with nitrogen at normal temperature are performed. The results of calculations are compared with available experimental data on nitrogen density variation in the jet. Satisfactory agreement of the results is obtained.

## 1 Introduction

Dozens of experimental and computational works are devoted to studies of the specific features of transcritical, near-critical, and supercritical fuel injection to a combustor [1]. Thus, presented in the review article [2] are the results of systematic experimental studies on the injection of cryogenic liquids (nitrogen and oxygen) as applied to liquid-propellant rocket engines implemented at the German Aerospace Center (DLR) (see, e. g., [3]) and in the U.S. Air Force Research Laboratory (AFRL) (see, e. g., [4]). An overview of the computational work is given, for example, in [5]. Calculations of sprays of cryogenic liquids are based on the equations of the real gas flow. Most often, the cubic EOS of the Peng–Robinson type are used with various corrections [6]. The flow equations are solved numerically, mainly, by the Large Eddy Simulation (LES) method [7] or Direct Numerical Simulation (DNS) [8], although the methods based on the solution of the Reynolds-averaged Navier–Stokes (RANS) equations are also used [9].

**DOI:** 10.30826/NEPCAP9B-27 

The objective of this work is to apply the analytical wide-range EOS of nitrogen developed in [10] to the gasdynamic calculation of submerged jets of cryogenic nitrogen.

## 2 Thermal Equations of State in the Single-Phase Regions of Nitrogen

According to [10], the thermal EOS for nitrogen in the single-phase regions of liquid, gas, and supercritical fluid is represented by the following formulae:

– at $\rho^g_{\rm tp} \leqslant \rho \leqslant \rho^l_{\rm tp}$,

$$P = P_s(\rho) + \rho f(\rho, T)\,[T - T_s(\rho)]\,\frac{R}{\mu}\,; \tag{1}$$

– at $0 \leqslant \rho \leqslant \rho^g_{\rm tp}$,

$$P = \rho f(\rho, T)\frac{R}{\mu}\,T\,. \tag{2}$$

Here, $R$ is the universal gas constant; $\mu$ is the molecular mass of nitrogen; $\rho^g_{\rm tp}$ and $\rho^l_{\rm tp}$ are the densities of gaseous and liquid nitrogen at the triple point ($\rho^g_{\rm tp}$ = 0.0006664 g/cm$^3$ and $\rho^l_{\rm tp}$ = 0.86722 g/cm$^3$); and $P_s(\rho)$ and $T_s(\rho)$ are the pressure and temperature at the nitrogen saturation line:

$$P_s(T) = \left[\left(\frac{T}{\alpha}\right)^{1/8} - A\right]^8\,; \quad T_s(\rho) = \alpha\left(P^{1/8} + A\right)^8$$

with

$$A = 6.07967\ \text{MPa}^{1/8},\ \alpha = 1.63514\cdot 10^{-5}\ \text{K at } 63.15 \leqslant T \leqslant 90\ \text{K}\,;$$
$$A = 5.75042\ \text{MPa}^{1/8},\ \alpha = 2.40954\cdot 10^{-5}\ \text{K at } 90 \leqslant T \leqslant 126.15\ \text{K}\,.$$

Function $f(\rho, T)$ in Eqs. (1) and (2) is represented as

$$f(\rho, T) = f(Z) = \sum_{i=0}^{5} a_i Z^i \tag{3}$$

with

$$Z = \frac{\rho}{\rho_c}\left(\frac{T^*}{T}\right)^{3/n(T,T^*)}\,,\ n(T,T^*) = B\left(\frac{T^*}{T}\right)^m\,,\ T^* = 400\ \text{K}$$

where $\rho_c$ is the critical density of nitrogen, and coefficients $a_i$, $B$, and $m$ are listed below: $a_0 = 1$; $a_1 = 0.9307944411889$; $a_2 = -0.7560883941$; $a_3$

$= 0.834935224625$; $a_4 = -0.278071370493$; $a_5 = 0.0415653559989$; $B = 22.6697273186$; and $m = -0.180648388772$.

The temperature in Eqs. (1) and (2) is limited from below by condition*:

$$T - T_s(\rho) \geqslant 0\,.$$

The value $\rho = \rho_{\rm tp}^g = 0.0006664$ g/cm$^3$ satisfies the equality:

$$P_s(\rho) - \frac{R}{\mu}\,\rho f(\rho, T) T_s(\rho) = 0\,.$$

## 3 Caloric Equations of State in the Single-Phase Regions of Nitrogen

The specific internal energy is the sum of the energy of an ideal gas

$$E^*(T) = \frac{5}{2}\,RT + \frac{R\theta}{\exp(\theta/T) - 1}\,, \quad \theta = 3340 \text{ K},$$

and excess energy $E_{\rm exc}$ determined by the integral:

$$E_{\rm exc} = \int\limits_0^\rho \left[P - T\left(\frac{\partial P}{\partial T}\right)_\rho\right] \rho^{-2}\, d\rho\,.$$

The caloric EOS in the three single-phase regions under consideration are expressed, respectively, by three different formulae, presented below [10]:

(1) liquid ($T \leqslant T_c$, $\rho_1(T) \leqslant \rho \leqslant \rho_{\rm tp}^l$)

$$E(\rho, T) = E_1 + \int\limits_{\rho_1(T)}^\rho \left[P - T\left(\frac{\partial P}{\partial T}\right)_\rho\right] \rho^{-2}\, d\rho\,,\ \rho_1(T) = \frac{1}{V_1(T)}\,; \qquad (4)$$

(2) gas ($T \leqslant T_c$, $0 \leqslant \rho \leqslant \rho_2(T)$)

$$E(\rho, T) = E_2 + \int\limits_{\rho_2(T)}^\rho \left[P - T\left(\frac{\partial P}{\partial T}\right)_\rho\right] \rho^{-2}\, d\rho\,,\ \rho_2(T) = \frac{1}{V_2(T)}\,; \qquad (5)$$

(3) supercritical fluid ($T > T_c$)

$$E(\rho, T) = E^0(T) + \int\limits_0^\rho \left[P - T\left(\frac{\partial P}{\partial T}\right)_\rho\right] \rho^{-2}\, d\rho \qquad (6)$$

*If condition (3) is violated, the system is in the two-phase region.

where $T_c$ is the critical temperature of nitrogen; $V$ is the specific volume; and indices 1 and 2 refer to the liquid and gas at the saturation line, respectively.

When calculating integrals (4)–(6), one should take into account the change in the thermal EOS of Eq. (1) during transitions through the density at the triple point.

## 4 Specific Heats of Nitrogen in the Single-Phase Regions

The relationship between the specific heat $C_v$ and the internal energy $E(\rho, T)$ is determined by the general formula:

$$C_v = \left(\frac{\partial E}{\partial T}\right)_v$$

in which $E$ in the cases of liquid, gas, and supercritical fluid is determined by Eqs. (4), (5), and (6), respectively. Moreover, in all three cases, in numerical calculations, the derivative $(\partial E/\partial T)_v$ can be replaced with a sufficient accuracy by the ratio of finite differences:

$$\left(\frac{\partial E}{\partial T}\right)_v = \lim_{\Delta T \to 0} \frac{E(T + \Delta T) - E(T)}{\Delta T} \tag{7}$$

with a sufficiently small value of $\Delta T$, for example, $0.00001T$.

In all three cases, the specific heat $C_p$ is calculated by the general formula:

$$C_p = C_V - T\frac{(\partial P/\partial T)_V^2}{(\partial P/\partial V)_T}$$

in which the derivatives $(\partial P/\partial T)_V$ and $(\partial P/\partial V)_T$ are calculated on the basis of thermal EOS of Eqs. (1) and (2). In numerical calculations, the derivatives can be replaced with a sufficient accuracy by the ratio of finite differences similarly to Eq. (7).

## 5 Statement of the Problem

Presented in [3] are the results of experiments on the injection of an axisymmetric jet of cryogenic nitrogen with an initial temperature $T_{\text{inj}}$ (120 and 130 K) and velocity $U_{\text{inj}}$ (from 1.8 to 5.4 m/s) into a cylindrical chamber filled with gaseous nitrogen at a pressure $P_0$ ranging from 3.95 to 5.98 MPa and room temperature $T_0 = 298$ K. The nozzle is a cylindrical circular channel with a diameter $D = 2.2$ mm and a length of 90 mm. The chamber has a diameter of 122 mm and a length of 1000 mm. In [3], the data are presented on the variation of the jet density along its axis and along the radius for 12 sets of outflow conditions. To demonstrate the applicability of the wide-range EOS of nitrogen [10], we use the results of [3], taking as a basis the following two sets of outflow conditions:

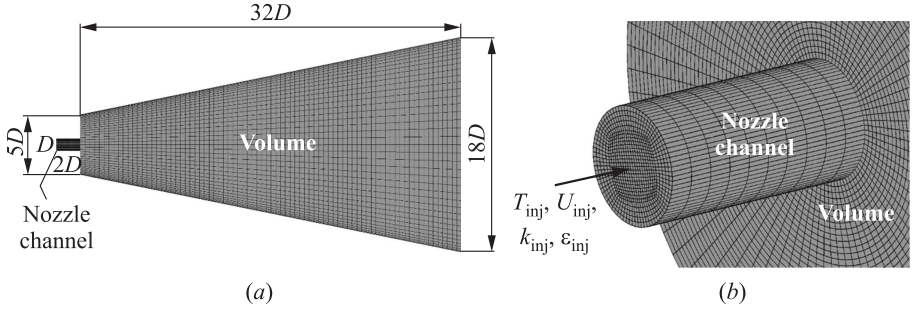


**Figure 1** Geometry of the computational domain: (*a*) side view; and (*b*) enlarged view from the side of the nozzle channel

(I) $T_{\text{inj}} = 126.9$ K; $U_{\text{inj}} = 4.9$ m/s; $P_0 = 3.97$ MPa; and $T_0 = 298$ K (run 3 in [3]); and

(II) $T_{\text{inj}} = 137$ K; $U_{\text{inj}} = 5.4$ m/s; $P_0 = 3.98$ MPa; and $T_0 = 298$ K (run 4 in [3]).

and solve the problem numerically using computational fluid dynamics methods. For doing so, we apply the problem statement from [8], in which the results of experiments [3] are compared with the results of DNS based on the Peng–Robinson EOS [6] with refinement [11].

Figure 1 shows the computational domain in the form of a short section of a nozzle channel with a diameter $D$ and length $2D$, through which a cryogenic nitrogen jet flows along the symmetry axis into a chamber. The chamber has the shape of an expanding truncated cone with a length of $32D$ with the minimum and maximum bases of diameters $5D$ and $18D$. The structured computational mesh contains 328,000 cells.

At the inlet to the nozzle channel, the temperature $T_{\text{inj}}$ and the velocity $U_{\text{inj}}$ of nitrogen are set as well as the turbulence parameters: kinetic energy $k_{\text{inj}}$ and its dissipation $\varepsilon_{\text{inj}}$ (the turbulent velocity and integral length scale were assumed to be $0.1U_{\text{inj}}$ and $0.1D$, respectively).

Constant pressure conditions $P_{\text{out}} = P_0$ are set at the outlet (right) section of the chamber. The wall of the nozzle channel and the left wall of the chamber are considered adiabatic and the side wall of the chamber is assumed to be isothermal with a temperature of 298 K.

The calculation is carried out using the AVL FIRE platform [12], into which the thermal and caloric EOS developed by us as well as the procedures for calculating the specific heat and molecular transport properties for nitrogen — viscosity and thermal conductivity — are preliminarily implemented. The coefficients of dynamic viscosity and thermal conductivity are calculated by the formulae [13]:

$$\eta = \eta_0(T) + \eta_r(T, \rho)\,; \tag{8}$$

$$\lambda = \lambda_0(T) + \lambda_r(T, \rho) + \lambda_c(T, \rho) \tag{9}$$

where $\eta_0$ is the coefficient of dynamic viscosity of nitrogen at low pressure; $\eta_r$ is the correction for the residual viscosity of liquid; $\lambda_0$ is the coefficient of thermal conductivity of nitrogen at low pressure; $\lambda_r$ is the correction for residual thermal conductivity; and $\lambda_c$ is the correction for thermal conductivity in the critical region.

For each term in Eqs. (8) and (9), there are corresponding relations and coefficients in [13]. The AVL FIRE platform is used worldwide for the design of reciprocating engines. The default thermal and caloric EOS in the code are the ideal-gas EOS. Earlier (in [14]), we used this code to perform comparative three-dimensional (3D) gasdynamic calculations of the operation process in the combustion chamber of a diesel engine using the ideal gas thermal and caloric EOS and the EOS of real gas, developed at the Federal Research Center for Chemical Physics of the Russian Academy of Sciences. A significant influence of the effects of real gas on the indicator diagram and on the yield of nitrogen oxides and soot was reported.

The numerical simulation of the injection of cryogenic nitrogen is performed using the 3D RANS equations, supplemented by the $k$–$\varepsilon$–$f$ turbulence model [15]. A segregated algorithm like semi-implicit method for pressure linked equations [16] is applied to solve the set of governing equations. Convective transport in the law of conservation of mass is approximated by the central difference, in the law of conservation of momentum by the total variation diminishing scheme with the MINMOD limiter [17], and for the rest of the equations, the standard UPWIND scheme of the first order is used.

## 6 Results of Calculations

Before gasdynamic calculations of the injection of a jet of cryogenic nitrogen into the volume, we verified all thermophysical parameters of the problem against the NIST (National Institute of Standards and Technology) database [18] on the isobar $P = 3.98$ MPa at $100 \leqslant T \leqslant 300$ K. Figure 2 shows the results of calculations for $C_p(T)$ (Fig. 2*a*), $\rho(T)$ (Fig. 2*b*), $E(T)$ (Fig. 2*c*), $\eta(T)$ (see Fig. 2*d*, Eq. (8)), and $\lambda(T)$ (see Fig. 2*e*, Eq. (9) with $\lambda_c = 0$). Note that the boiling point of nitrogen at a pressure of $P = 3.98$ MPa is 130 K. At this temperature, the specific heat $C_p$ has a pronounced local maximum. Comparison shows that in the indicated temperature range, all the thermophysical parameters of the problem, obtained by the proposed EOS and by Eqs. (8) and (9), are in excellent agreement with the data [18].

The results of gasdynamic calculations are presented in Figs. 3 to 5. Figure 3 shows the steady-state fields of nitrogen density in the longitudinal section

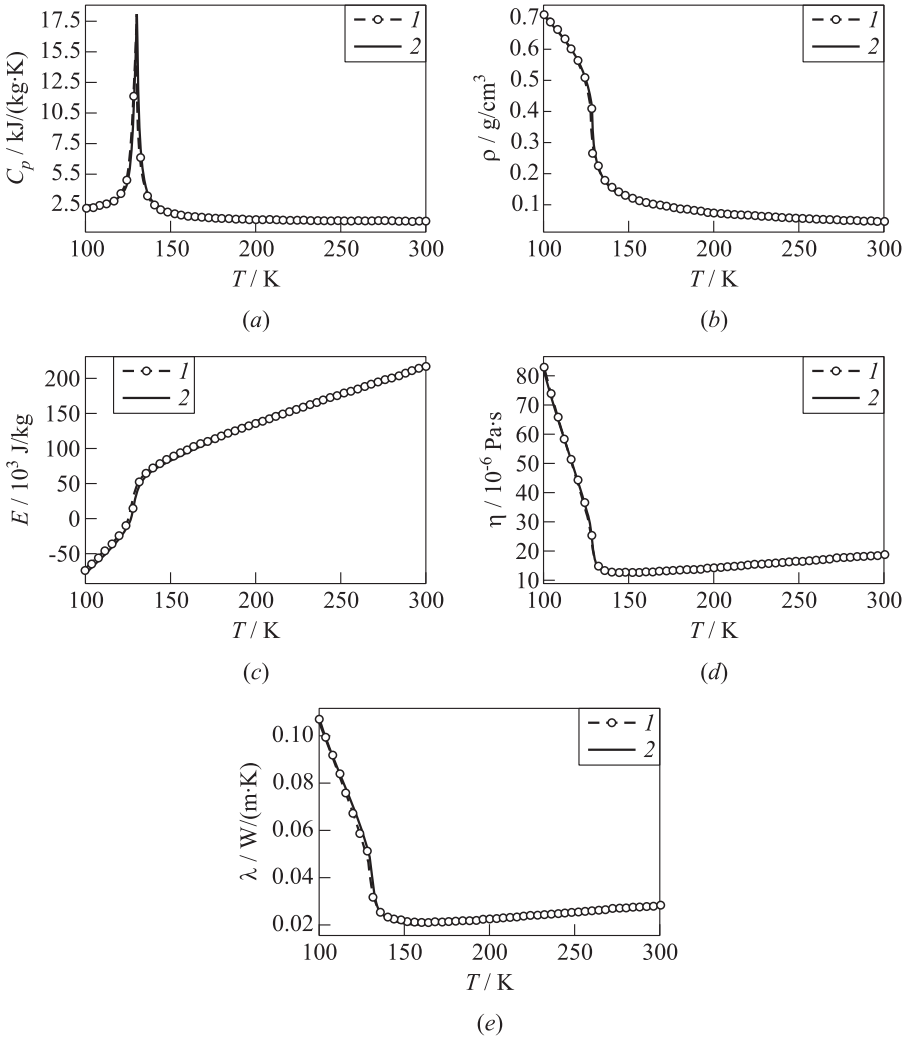


**Figure 2** Comparison of the calculated (*1*) dependences $C_p(T)$ (*a*), $\rho(T)$ (*b*), $E(T)$ (*c*), $\eta(T)$ (*d*), and $\lambda(T)$ (*e*) with the data of [18] (*2*) for nitrogen at isobar 3.98 MPa

of the computational domain, obtained for sets of conditions I and II. Figure 4 compares the calculated and measured in [3] dependences of the nitrogen density on the dimensionless distance to the nozzle exit $X/D$ along the axis of symmetry of the jet for the same sets of conditions. Finally, Fig. 5 compares the calculated and measured in [3] radial profiles of nitrogen density at different values of $X/D$

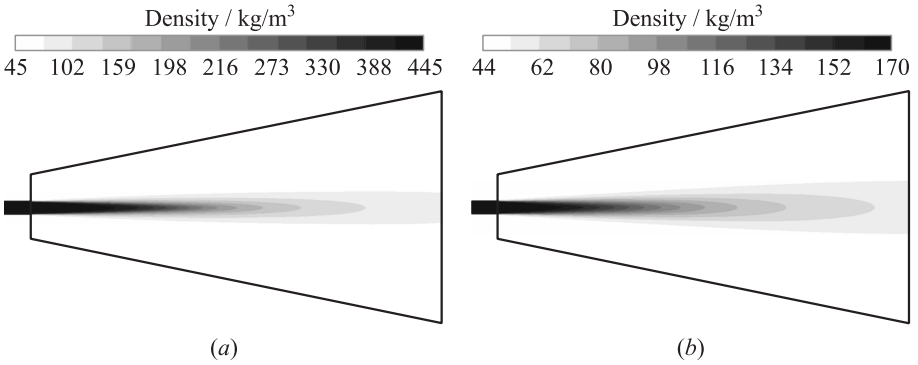


**Figure 3** Calculated fields of nitrogen density in the longitudinal section of the computational domain obtained for sets of conditions I ($a$) and II ($b$)

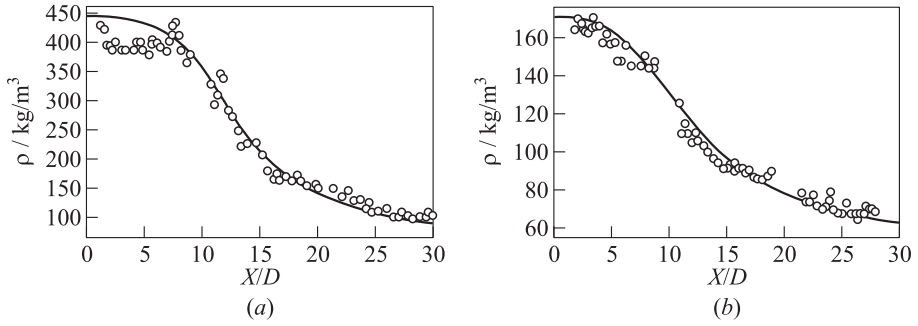


**Figure 4** Comparison of the calculated (curves) and measured [3] (symbols) profiles of nitrogen density along the axis of symmetry of the jet for sets of conditions I ($a$) and II ($b$)

(from 1.2 to 25) for a set of conditions I. Moreover, in accordance with [3], the dimensionless density $\rho_+$ is defined as

$$\rho_+ = \frac{\rho - \rho_0}{\rho_a - \rho_0}$$

where $\rho_0$ is the initial nitrogen density in the chamber; $\rho_a$ is the nitrogen density at the jet axis; and the radius $r$ is related to the radius $r_{1/2}$, at which the nitrogen density is equal to the mean arithmetic value $\rho_{1/2} = (\rho_a + \rho_0)/2$.

It follows from Fig. 4 that the calculation reproduces the steady-state density distributions along the jet axis for both sets of conditions within the experimental error. As for the radial density distributions in Fig. 5, at $X/D \leqslant 5$, $X/D = 15$, and $X/D = 25$, the calculation reproduces well the experimental data, giving

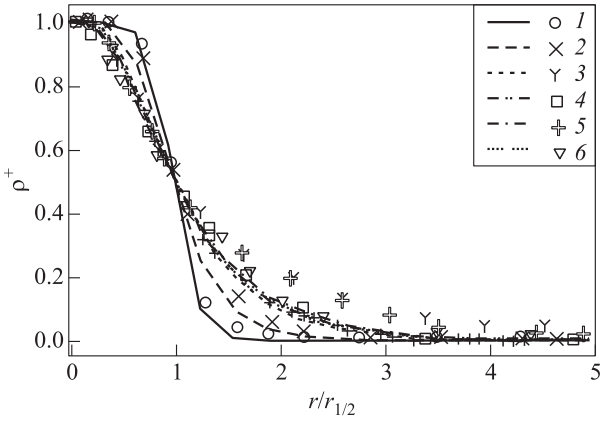


**Figure 5** Comparison of the calculated (curves) and measured [3] (symbols) distributions of the dimensionless density of nitrogen on the dimensionless radius $r/r_{1/2}$ at different distances from the nozzle exit $X/D$ for a set of conditions I: *1* — $X/D = 1.2$; *2* — 5; *3* — 10; *4* — 15; *5* — 20; and *6* — $X/D = 25$

the jet width values close to the measured ones. However, at $X/D = 10$ and 20, the calculation underestimates the density at the jet periphery. This latter effect can be associated with the presence of large eddies in the jet structure which are not resolved by the turbulence model used.

## 7 Concluding Remarks

Thus, the analytical wide-range EOS of nitrogen developed in [10] has been implemented into the gasdynamic code for calculating the injection of a dense submerged turbulent jet of cryogenic nitrogen into a chamber filled with nitrogen at normal temperature and pressure of 3.98 MPa. The results of calculations are compared with the experimental data on the variation of the density of matter in jets of cryogenic nitrogen of the initial supercritical temperature (126.9 and 137 K). Satisfactory agreement of the results is obtained.

## Acknowledgments

This research work was performed at the expense of a subsidy allocated by the Semenov Federal Research Center for Chemical Physics of the Russian Academy of Sciences to implement the State Task on the topic No. 0082-2019-0006 (Registration No. AAAA-A21-121011990037-8) and by the Federal State Institution "Scientific Research Institute for System Analysis of the Russian Academy of

Sciences" to implement the State Task on the topic No. 0065-2019-0005 (Registration No. AAAA-A19-119011590092-6).

## References

1. Ashgriz, N., ed. 2011. *Handbook of atomization and sprays: Theory and applications*. New York, NY: Springer. 951 p. doi: 10.1007/978-1-4419-7264-4.
2. Oschwald, M., J. J. Smith, R. Branam, J. Hussong, A. Schik, B. Chehroudi, and D. Talley. 2006. Injection of fluids into supercritical environments. *Combust. Sci. Technol.* 178(1-3):49–100. doi: 10.1080/00102200500292464.
3. Mayer, W., J. Tellar, R. Branam, G. Schneider, and J. Hussong. 2003. Raman measurement of cryogenic injection at supercritical pressure. *Heat Mass Transfer* 39:709–719.
4. Chehroudi, B., and D. Talley. 2004. Fractal geometry of a cryogenic nitrogen round jet injected into sub- and super-critical conditions. *Atomization Spray.* 14:81–91.
5. Zong, N., and V. Yang. 2006. Cryogenic fluid jets and mixing layers in transcritical and supercritical environments. *Combust. Sci. Technol.* 178:193–227. doi: 10.1080/00102200500287613.
6. Peng, D. Y., and D. P. Robinson. 1976. A new two-constant equation of state. *Ind. Eng. Chem. Fund.* 15(1):59–64. doi: 10.1026/l160057a011.
7. Jarczyk, M., and M. Pitznery. 2012. Large eddy simulation of supercritical nitrogen jets. AIAA Paper No. 2012-1270.
8. Ries, F., P. Obando, I. Shevchuck, J. Janicka, and A. Sadiki. 2017. Numerical analysis of turbulent flow dynamics and heat transport in a round jet at supercritical conditions. *Int. J. Heat Fluid Fl.* 66:172–184. doi: 10.1016/j.ijheatfluidflow.2017.06.007.
9. Sierra-Pallares, J., J. Garcia del Valle, P. Garcia-Carrascal, and F. Castro Ruiz. 2016. Numerical study of supercritical and transcritical injection using different turbulent Prandlt numbers: A second law analysis. *J. Supercrit. Fluid.* 115:86–98. doi: 10.1016/j.supflu.2016.05.001.
10. Kuznetsov, N. M., S. N. Medvedev, S. M. Frolov, F. S. Frolov, B. Basara, and K. Pachler. 2020. Termicheskoe i kaloricheskoe uravneniya sostoyaniya azota v shirokom diapazone plotnosti i temperatury: primenenie k raschetam istecheniya kriogennykh struy [Thermal and caloric equations of state for nitrogen in a wide range of density and temperature: Application to calculation of cryogenic jet injection]. *Goren. Vzryv (Mosk.) — Combustion and Explosion* 13(2):118–131. doi: 10.30826/CE20130213.
11. Abudour, A. M., S. A. Mohammad, R. L. Robinson, Jr., and K. A. M. Gasem. 2012. Volume-translated Peng–Robinson equation of state for saturated and single-phase liquid densities. *Fluid Phase Equilibr.* 335:74–87. doi: 10.1016/j.fluid.2012.08.013.
12. AVL FIREr — Computational Fluid Dynamics for Conventional and Alternative Powertrain Development. Available at: https://www.avl.com/fire (accessed March 31, 2021).
13. Lemmon, E. W., and R. T. Jacobsen. 2004. Viscosity and thermal conductivity equations for nitrogen, oxygen, argon, and air. *Int. J. Thermophys.* 25(1):21–69.

14. Frolov, S. M., V. S. Ivanov, R. R. Tukhvatullina, F. S. Frolov, N. M. Kuznetsov, and B. Basara. 2019. Raschet rabochego protsessa v dizele s uravneniem sostoyaniya real'nogo gaza [Numerical simulation of the operation process in a diesel engine with the real-gas equation of state]. *Goren. Vzryv (Mosk.) — Combustion and Explosion* 12(1):73–83 doi: 10.30826/CE19120109.
15. Hanjalic, K., M. Popovac, and M. Hadziabdic. 2004. A robust nearwall elliptic relaxation eddy-viscosity turbulence model for CFD. *Int. J. Heat Fluid Fl.* 25:897–901.
16. Ferziger, J. H., and M. Peric. 1996. *Computational methods for fluid dynamics*. New York, NY: Springer-Verlag. 370 p.
17. Sweby, P. K. 1984. High resolution schemes using flux limiters for hyperbolic conservation laws. *SIAM J. Numer. Anal.* 21(5):995. doi: 10.1137/0721062.
18. Lemmon, E. W., M. O. McLinden, and D. G. Friend. Thermophysical properties of fluid systems. *NIST Chemistry WebBook, NIST Standard Reference Database Number 69*. Eds. P. J. Linstrom, and W. G. Mallard. Gaithersburg, MD: National Institute of Standards and Technology. doi: 10.18434/T4D303.

# СВЕРХКРИТИЧЕСКОЕ ИСТЕЧЕНИЕ КРИОГЕННОЙ СТРУИ АЗОТА

**Н. М. Кузнецов**[1], **С. Н. Медведев**[1], **С. М. Фролов**[1,2,3], **Ф. С. Фролов**[1,3], **Б. Басара**[4], **К. Пахлер**[4]

[1]Федеральный исследовательский центр химической физики им. Н. Н. Семёнова Российской академии наук (ФИЦ ХФ РАН)
Россия, Москва 119991, ул. Косыгина, д. 4
[2]Национальный исследовательский ядерный университет МИФИ
Россия, Москва 115409, Каширское ш., д. 31
[3]Федеральное государственное учреждение «Федеральный научный центр Научно-исследовательский институт системных исследований Российской академии наук» (ФГУ ФНЦ НИИСИ РАН)
Россия, Москва 117218, Нахимовский просп., д. 36, корп. 1
[4]АВЛ Лист ГмбХ
Грац, Австрия

Аналитическое уравнение состояния (УрС) реального газа для азота, справедливое в широком диапазоне плотности (от 0 до плотности жидкости в тройной точке: 0,867 г/см$^3$) и температуры (от 100 до 5000 K), внедрено в газодинамическую программу для расчета многомерных турбулентных реагирующих течений. С использованием нового УрС проведены расчеты истечения плотной затопленной турбулентной струи криогенного азота в ка-

меру, заполненную азотом при нормальной температуре. Проведено сравнение результатов расчетов с экспериментальными данными по изменению плотности вещества в струе. Получено удовлетворительное согласие результатов. Разработанное УрС позволяет разделять области жидкости и газа по локальным мгновенным значениям плотности и температуры в струе без применения модели двухфазного течения.

Работа выполнена за счет субсидии, выделенной ФИЦ ХФ РАН на выполнение государственного задания по теме 0082-2016-0011 (номер государственной регистрации АААА-А17-117040610346-5), и субсидии, выделенной ФГУ ФНЦ НИИСИ РАН по теме 0065-2019-0005 (номер государственной регистрации АААА-А19-119011590092-6).